Journal of
Synchrotron
Radiation

ISSN 1600-5775

Received 9 December 2013
Accepted 27 March 2014

Spectral modulation of higher harmonic spontaneous emission from an optical klystron

Norihiro Sei,[a]* Hiroshi Ogawa,[a] Kawakatsu Yamada,[a] Masaki Koike[a] and Hideaki Ohgaki[b]

[a]Research Institute of Instrumentation Frontier, National Institute of Advanced Industrial Science and Technology, 1-1-1 Umezono, Tsukuba, Ibaraki 305-8568, Japan, and [b]Institute of Advanced Energy, Kyoto University, Gokanosho, Uji, Kyoto 611-0011, Japan. *E-mail: sei.n@aist.go.jp

Higher harmonics of spontaneous emission from an optical klystron have been observed. The modulation factor of the spontaneous emission spectrum for the higher harmonics can be described by considering the observation system. When the dispersive gap of the optical klystron was fixed, the microstructure interval of the spontaneous emission spectrum at a certain resonant wavelength became narrower as the order of the higher harmonic became larger. Some unique characteristics of the higher harmonics have been clarified, and these studies are likely to contribute to the development of free-electron lasers using higher harmonics of an optical klystron in the shorter-wavelengths region.

Keywords: free-electron laser; optical klystron; spontaneous emission; higher harmonic; spectrum.

1. Introduction

Optical klystrons generate modulated spontaneous emission by using the phase difference between two undulator sections. Although the energy spread of an electron beam has to be narrow in order to oscillate a free-electron laser (FEL) with an optical klystron, the optical klystron can achieve a high FEL gain given its length. Thus, optical klystrons have been used as an insertion device for the whole storage-ring FEL system (Deacon *et al.*, 1984; Litvinenko, 1988; Couprie *et al.*, 1991; Takano *et al.*, 1993; Yamazaki *et al.*, 1993; Litvinenko *et al.*, 1999; Walker *et al.*, 2001) and have contributed to shorten the FEL wavelength down to the vacuum-ultraviolet region (Litvinenko *et al.*, 2001; Marsi *et al.*, 2002). The characteristics of the optical klystron's spontaneous emission were analyzed by the Novossibirsk group and by the ACO group (Elleaume, 1984*a*; Vinokurov & Skrinskii, 1977), and these groups reported the results of detailed measurements of the fundamental harmonic spontaneous emission. A helical-type optical klystron, which could control polarization of a FEL, was developed by the UVSOR group (Hama *et al.*, 1997).

Higher harmonics of spontaneous emission from an optical klystron have been used for developing the shorter-wavelength coherent light sources since the development of the fundamental harmonic storage-ring FELs. Coherent harmonic generation (CHG) is a phenomenon that describes how a high-peak-power laser, having the same wavelength as the fundamental harmonic of an optical klystron, induces density modulation on an electron bunch in the optical klystron and the electron bunch emits high-power higher harmonics from the optical klystron. In 1984, the ACO group reported observations of ultraviolet CHG that were made by using an yttrium aluminium garnet laser injected into the optical klystron, synchronized with the electron bunch (Girard *et al.*, 1984). Secondary to this achievement, some groups developed CHGs in the vacuum-ultraviolet region (Prazeres *et al.*, 1988, 1991; Litvinenko, 2003). Recently, owing to the development of short-pulse and high-power lasers, it became possible to obtain the CHG with a pulse energy of tens of pJ in the ultraviolet region (Labat *et al.*, 2007; Khan *et al.*, 2011). On the other hand, higher harmonic oscillations in FELs were also achieved in many FEL facilities (Benson & Madey, 1989; Warren *et al.*, 1990; Neil *et al.*, 2001; Kubarev *et al.*, 2011). The higher harmonic oscillation using an optical klystron was reported by the Duke group for the first time (Wu *et al.*, 2008). We demonstrated FEL oscillations using up to the seventh harmonic with the optical klystron ETLOK-III in the infrared FEL system of the storage ring NIJI-IV (Sei *et al.*, 2010, 2012*a*). The seventh-harmonic FEL oscillation was the highest harmonic order ever achieved for the higher harmonic FEL oscillations. We also achieved visible FEL oscillations with the third harmonic in the NIJI-IV infrared FEL system (Sei *et al.*, 2012*b*), and it was then verified that higher harmonics were useful in shortening the wavelength of FEL oscillations.

However, except for some early pioneering studies, no detailed investigations have been performed yet to study the spectra of an optical klystron's higher harmonic spontaneous emission (Deacon *et al.*, 1984; Billardon *et al.*, 1983). As the order of the harmonic increases, it becomes more difficult to precisely measure the spectrum of the optical klystron's higher harmonic spontaneous emission because its modulation becomes less distinctive. To reveal the higher harmonic FEL

oscillations, it becomes important to detect the higher harmonic spontaneous emission of the optical klystron. Thus, we prevented the degradation of spectral modulation of higher harmonic spontaneous emission by adjusting the gap in the dispersive section in the ETLOK-III, and were able to precisely measure the spectrum of the higher harmonic spontaneous emission. We gained some novel insights regarding the higher harmonic spontaneous emission of the optical klystron, and we report our findings in this article.

2. The optical klystron ETLOK-III

A planar optical klystron ETLOK-III was incorporated into the infrared FEL system as an insertion device (Sei *et al.*, 2002). It had two identical undulator sections of 1.4 m length and one dispersive section of 0.72 m length. The undulator period in the undulator section λ_u was 0.2 m, and the number of periods N_u was 7. The gap of the undulator section g_u could be adjusted to be between 36 and 150 mm, and then the value of the deflection parameter K varied from 1.28 to 10.4. Because the stage that supported the magnets of the dispersive section was put between the stages that supported the magnets of the undulator sections, the gap of the dispersive section g_d could be made at most 38 mm wider than g_u. However, g_d could be changed independently of g_u, and its value ranged from 42 to 188 mm (Sei *et al.*, 2008). It was possible to investigate the influence of the dispersive section on the FEL gain and power without changing the conditions of the electron beam and the undulator section. Because the FEL experiments were conducted with an electron beam energy of 310 MeV (Sei *et al.*, 2009, 2011), the higher harmonic spontaneous emission of the ETLOK-III could be observed in the near-infrared and visible regions. Therefore, it was easy to measure the spectrum of the higher harmonic spontaneous emission. We have developed the third-harmonic FEL oscillations in a wide range of wavelengths, from 549 to 1551 nm (Sei *et al.*, 2012*c*).

3. The microstructure of the optical klystron's spontaneous emission spectrum

When a bunch of electrons passes through the first undulator section of the optical klystron, it interacts with the optical pulse beam and velocity modulation is generated in the bunch of electrons. This velocity modulation is converted into the density modulation of the bunch in the dispersive section because the electrons travel through it in a curved orbit. The efficiency of this conversion depends on the number of periods of the fundamental harmonic wavelength passing over an electron in the dispersive section, N_d, which is given by

$$N_d = \frac{d}{2\lambda_{R1}\gamma^2}\left\{1+(\gamma\theta)^2+\frac{e^2}{m^2c^2d}\int_{-\infty}^{\infty}\left[\int_{-\infty}^{u}B_d(z)\,dz\right]^2 du\right\}, \quad (1)$$

where m, e, c, θ and γ are the electron mass, electron charge, speed of light, observation angle relative to the electron beam axis, and the electron energy in units of its rest mass (Deacon *et al.*, 1984), respectively. The parameter d is the length of the dispersive section, and $B_d(z)$ is the vertical magnetic field on the electron beam axis, created by the dispersive section magnet at the longitudinal coordinate z. The parameter λ_{R1} denotes the resonant wavelength of the fundamental harmonic spontaneous emission, and for the nth order it is given by the following equation,

$$\lambda_{Rn} = \frac{\lambda_u}{2n\gamma^2}\left[1+\frac{K^2}{2}+(\gamma\theta)^2\right]. \quad (2)$$

This delay of the electron with respect to the spontaneous emission of the first undulator causes a phase shift for the spontaneous emission of the second undulator. This phase shift is responsible for generating the modulation in the optical klystron's spontaneous emission spectrum. By neglecting the radiation from the dispersive section, the optical klystron's spontaneous emission spectrum for a wavelength λ is given by

$$S_{OK}(\lambda) = 2S_{und}(\lambda)\left\{1+f\cos\left[2\pi n(N_u+N_d)\frac{\lambda_{Rn}}{\lambda}\right]\right\}, \quad (3)$$

where f is the modulation factor, and the symbol S_{und} stands for the spontaneous emission spectrum of the undulator section (Elleaume, 1984*a*; Billardon *et al.*, 1985). For a planar undulator, S_{und} in the perpendicular plane including the electron beam axis is given by

$$S_{und}(\lambda) = \frac{(eK\gamma nN_u)^2}{4\varepsilon_0\lambda^2\left[1+(K^2/2)+(\gamma\theta)^2\right]^2}\left(\frac{\sin\delta_\lambda}{\delta_\lambda}\right)^2 \times\left[J_{(n-1)/2}(n\xi)-J_{(n+1)/2}(n\xi)\right]^2, \quad (4)$$

$$\xi = \frac{K^2}{4+2K^2+4(\gamma\theta)^2}, \quad (5)$$

$$\delta_\lambda = \pi N_u n\left(\frac{\lambda_{Rn}}{\lambda}-1\right), \quad (6)$$

where ε_0 is the permittivity of free space, and the order n is limited to positive odd numbers (Brau, 1990). Fig. 1 shows the radiation profile of the spontaneous emission from ETLOK-III, measured by a charge-coupled device camera at g_u = 86 mm (K = 4.23) and g_d = 120 mm. An aperture, which was set at a distance of 7.6 m from the center of ETLOK-III and had an opening of 35 mm, was used in this observation. According to equation (2), the resonant wavelength of the fundamental harmonic spontaneous emission was approximately 2.71 µm, so that only the fifth-harmonic spontaneous emission was emitted on the electron beam axis in the visible region. It is noted that the fifth-harmonic spontaneous emission varies from green to red in Fig. 1 as the observation angle becomes larger. All of the even harmonics of the spontaneous emission vanish identically in the perpendicular plane including the electron beam axis, but they appear in the horizontal plane

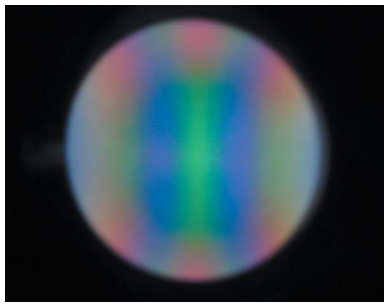

Figure 1
Photograph of the spontaneous emission profile from the optical klystron ETLOK-III at g_u = 86.0 mm (K = 4.23) and g_d = 120 mm. An aperture with an opening of 35 mm was placed 7.6 m from the center of the ETLOK-III.

when $\theta > 0$ (Yoshikawa *et al.*, 1994). As shown in Fig. 1, the sixth-harmonic spontaneous emission was observed as the vertical blue stripes. Equations (3) and (4) show that the envelope of the optical klystron spectrum is determined by $(\sin\delta_\lambda/\delta_\lambda)^2$. As an ordinary planar undulator, this factor results in the narrowing of the width of the envelope of the higher harmonic spontaneous emission spectrum. Fig. 2 shows spectra of the third-harmonic and fifth-harmonic spontaneous emission at g_u = 87.8 mm (K = 4.10) and g_d = 120 mm. Compact spectrometers with resolutions of 0.83 and 0.24 nm were used to measure the third and the fifth harmonics, respectively. The measured envelope width of spontaneous emission was 38.0 nm for the third harmonic in full width at half-maximum (FWHM). The ideal envelope width calculated with a single-electron beam was 36.2 nm. The spectrum of the third-harmonic spontaneous emission became slightly wider due to the electron-beam emittance. The measured envelope width of spontaneous emission was 12.7 nm for the fifth harmonic FWHM. The width ratio of the third to fifth harmonics was 2.99, and it was almost in accord with the theoretical value of $(5/3)^2$.

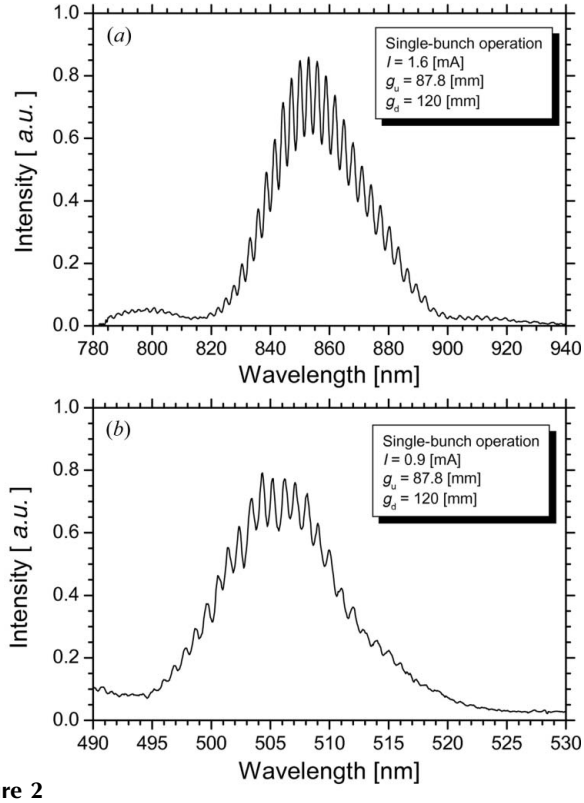

Figure 2
Measured spectra of the third harmonic (*a*) and the fifth harmonic (*b*) spontaneous emission at g_u = 87.8 mm (K = 4.10) and g_d = 120 mm. Compact spectrometers with resolutions of 0.83 and 0.24 nm were used in (*a*) and (*b*), respectively. The electron beam current in a single-bunch operation was 1.6 mA in (*a*) and 0.9 mA in (*b*).

As shown in equation (3), the parameter N_d characterizes the modulation that appears in the optical klystron's spontaneous emission spectrum (Sei *et al.*, 2007). The microstructure interval $\Delta\lambda_n$ for the nth harmonic spontaneous emission spectrum is given by

$$\Delta\lambda_n \cong \frac{\lambda_{Rn}}{n(N_u + N_d)}. \quad (7)$$

Thus, we can expect the relationship $\Delta\lambda_m/\Delta\lambda_n = (n/m)^2$ to hold. In Fig. 2, the measured values of $\Delta\lambda_3$ and $\Delta\lambda_5$ were 2.97 and 1.06 nm, respectively. This confirms that the ratio of $\Delta\lambda_3$ to $\Delta\lambda_5$ is almost in accord with the theoretical value of $(5/3)^2$.

Equation (3) also shows that $\Delta\lambda_n$ depends on the higher harmonic order, even for the same resonant wavelength. By definition of N_d, the quantity nN_d does not depend on the higher harmonic order at a resonant wavelength. However, the quantity nN_u does depend on the higher harmonic order, thus $\Delta\lambda_n$ changes with the harmonic order. As with the optical klystron OK-4 in the Duke FEL Laboratory (Litvinenko *et al.*, 1999), because the ETLOK-III could change the K value of the undulator section with fixed magnetic field in the dispersive section we could measure the dependence of $\Delta\lambda_n$ on the order of the higher harmonic. Fig. 3 shows the spontaneous emission spectra of the fundamental and third harmonics with g_d = 120 mm, obtained when the resonant wavelength was adjusted to approximately 855 nm. In these measurements, dielectric multilayer mirrors whose reflectance had a maximum at the wavelength of approximately 855 nm were installed in the mirror cavities of the infrared FEL system. The transmittance of the mirror (0.02%) was hardly dependent on the wavelength around the target wavelength of 855 nm; thus, the mirror did not influence the evaluation of $\Delta\lambda_n$. The measured microstructure intervals were 3.12 nm for the fundamental harmonic and 2.96 nm for the third harmonic, respectively. By using equation (7), the difference of $\lambda_{R3}/\Delta\lambda_3 - \lambda_{R1}/\Delta\lambda_1$ was evaluated to be 14.8, which was almost in accord with the theoretical value of $2N_u$.

Moreover, we measured $\Delta\lambda_n$ by observing spectra of higher harmonic spontaneous emission at the wavelength of approximately 890 nm in the FEL experiments (Sei *et al.*, 2012*a*). Fig. 4 shows the $\lambda_{Rn}/\Delta\lambda_n$ ratio, evaluated by the measured $\Delta\lambda_n$ for the fundamental, third, fifth and seventh harmonics. The tunable range of the dispersive gap of ETLOK-III was limited by the undulator section, and we could not measure $\Delta\lambda_n$ for all of the higher harmonic orders at the same g_d. However, by fitting the $\lambda_{Rn}/\Delta\lambda_n$ values that were measured for the third harmonic to an exponential function,

Table 1
Comparison of the measured $\lambda_{Rn}/\Delta\lambda_n$ with the fitting curve results for the third harmonic, and the measured $\lambda_{Rn}/\Delta\lambda_n$ for the other harmonic orders.

Dispersive gap, g_d (mm)	$\lambda_{Rn}/\Delta\lambda_n$ for third harmonic in fitting curve	Compared order of harmonic	$\lambda_{Rn}/\Delta\lambda_n$ for the measurement data	Difference between the measurement and fitting curve
100	394.6	7	422.6	+28.0
109	335.4	5	350.2	+14.8
125	252.4	1	235.9	−16.5

the ratio $\lambda_{Rn}/\Delta\lambda_n$ for the third harmonic could be compared with the ratios obtained for other order harmonics, as listed in Table 1. It is noted that the value of $\lambda_{Rn}/\Delta\lambda_n$ at the same g_d and same wavelength was found to depend on the order of the higher harmonic. We experimentally clarified, for the first time, the dependence of $\Delta\lambda_n$ on the higher harmonic order.

4. Observation of the modulation factor for the higher harmonics

The modulation factor f, which expresses the modulation rate of the spectral microstructure, is affected by several different physical parameters. For storage rings, the measured f is simply the product of three individual f factors, namely,

$$f = f_e f_f f_m, \tag{8}$$

where f_e is the modulation factor due to the multi-electron emission, f_f is contributed by the optical klystron field imperfection, and f_m is that due to the observation (Deacon *et al.*, 1984; Elleaume, 1984*a*). Generally, the factor f_f only insignificantly contributes to the degradation of f.

The factor f_e also consists of three factors: the energy spread of the electron beam, size of the electron beam and angular divergence of the electron beam. The main contribution to f_e comes from the energy spread σ_γ, and the factor due to the energy spread for the fundamental harmonic, $f_{\gamma 1}$, is given by

$$f_{\gamma 1} = \exp\left[-8\pi^2 \left(N_u + N_d\right)^2 \left(\sigma_\gamma/\gamma\right)^2\right]. \tag{9}$$

This formula was derived by accounting for the phase distribution of the cosine function in equation (3), which was caused by the energy spread. Then, the factor for the nth harmonic, $f_{\gamma n}$, is obtained by replacing $N_u + N_d$ with $n(N_u + N_d)$ in equation (9), namely (Sei *et al.*, 2010)

$$f_{\gamma n} = \exp\left[-8\pi^2 n^2 \left(N_u + N_d\right)^2 \left(\sigma_\gamma/\gamma\right)^2\right]. \tag{10}$$

For the FEL experiments in the NIJI-IV, the energy spread of the electron beam was evaluated to be 4.0×10^{-4} (Sei *et al.*, 2010). The optimized value of $n(N_u + N_d)$, which maximized the FEL gain with ETLOK-III, was approximately 200 (Couprie *et al.*, 1989).

Although f_m does not contribute to the reduction of the FEL gain, an observed optical klystron's spontaneous emission spectrum includes degradation of the modulation due to f_m. To evaluate the FEL gain precisely, it is important to remove f_m from the measured f. According to the literature, f_m for the fundamental harmonic, f_{m1}, is given by

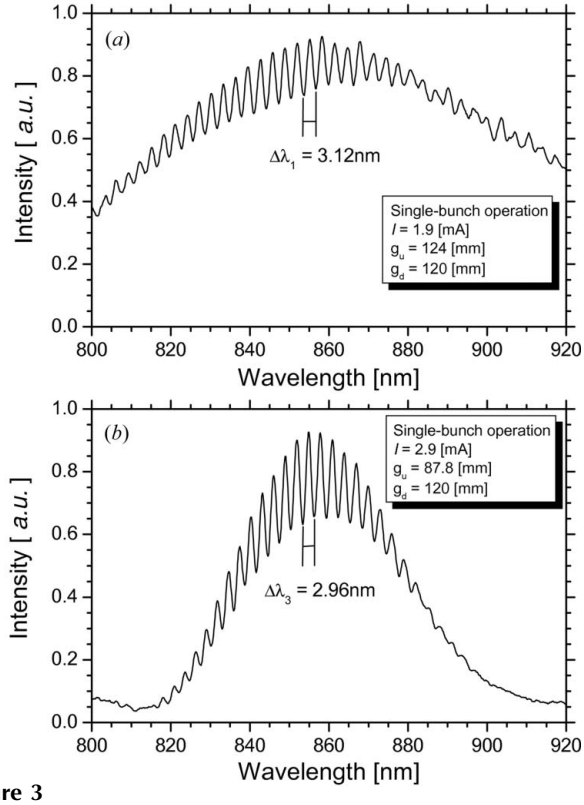

Figure 3
Measured spectra of the fundamental harmonic (*a*) and the third harmonic (*b*) spontaneous emission with g_d = 120 mm at the resonant wavelength of ∼855 nm. The undulator gaps were 124 mm (K = 2.07) for the fundamental harmonic and 87.8 mm (K = 4.10) for the third harmonic. The electron beam current in a single-bunch operation was 1.9 mA in (*a*) and 2.9 mA in (*b*).

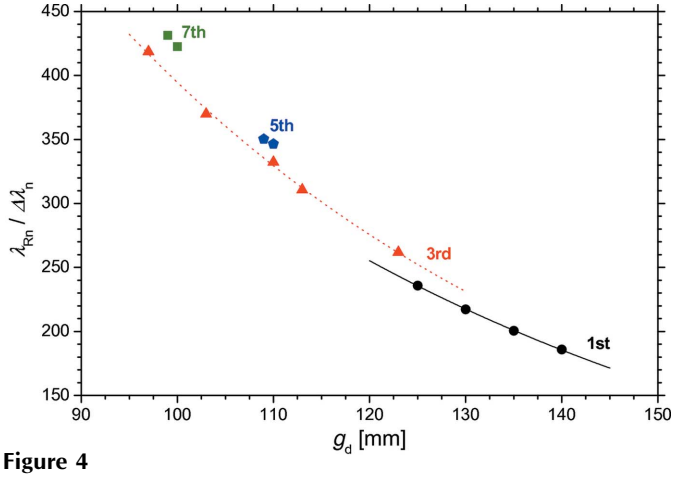

Figure 4
Evaluated values of $\lambda_{Rn}/\Delta\lambda_n$ obtained from the measurements of $\Delta\lambda_n$ for the fundamental (K = 2.13), third (K = 4.19), fifth (K = 5.52) and seventh harmonics (K = 6.62) at the resonant wavelength of ∼890 nm. The dotted and solid lines are the exponential fitting curves for the fundamental and third harmonics, respectively.

Table 2
Measured and calculated values of the modulation factors for the fundamental and third harmonics.

Order of harmonic, n	Measured modulation factor, f	Calculated modulation factor due to energy spread, f_γ	Calculated modulation factor due to observation, f_m	Ratio of measurement to calculation, $f_\gamma f_\mathrm{m}/f$
1	0.428	0.646	0.696	0.951
3	0.283	0.378	0.762	0.983

$$f_{\mathrm{m}1} = \exp\left[-\left(\frac{\pi}{12}\frac{L+d}{\lambda}a^2\right)^2\right]\frac{\sin^2\alpha_1}{\alpha_1^2}, \tag{11}$$

$$\alpha_1 = \pi\left(N_\mathrm{u}+N_\mathrm{d}\right)\frac{\Delta\lambda}{\lambda}, \tag{12}$$

where L is the length of one undulator section, a is the total angular aperture of the pinhole, and $\Delta\lambda$ is the resolution of the detector in FWHM (Vinokurov & Skrinskii, 1977; Billardon *et al.*, 1983). The first and second factors on the right-hand side in equation (11) represent the influences due to the observation angle and the resolution of the measuring system, respectively. By using equation (2), a variation in the wavelength of the nth harmonic spontaneous emission, $\delta\lambda$, which is caused by a slight observation angle $\delta\theta$ relative to the electron beam axis, is given by

$$\delta\lambda = (\lambda_\mathrm{u}/2n)(\delta\theta)^2. \tag{13}$$

In the case of $\lambda_{\mathrm{R}n} = \lambda_{\mathrm{R}1}$, this relationship indicates that the observation angle that is necessary to obtain a certain wavelength shift is proportional to $n^{1/2}$ for the nth harmonic spontaneous emission. Then, the first factor on the right-hand side in equation (11) changes, for the nth harmonic spontaneous emission, and becomes

$$\exp\left[-\left(\frac{\pi}{12}\frac{L+d}{n\lambda}a^2\right)^2\right]. \tag{14}$$

The factor α_1 is derived by considering the phase distribution of the cosine function in equation (3), similar to what was obtained for f_γ. For the nth harmonic spontaneous emission, equation (12) can be simply expanded as follows,

$$\alpha_n = \pi n\left(N_\mathrm{u}+N_\mathrm{d}\right)\Delta\lambda/\lambda. \tag{15}$$

Therefore, the observation-related modulation factor for the nth harmonic spontaneous emission, $f_{\mathrm{m}n}$, is expressed as

$$f_{\mathrm{m}n} = \exp\left[-\left(\frac{\pi}{12}\frac{L+d}{n\lambda}a^2\right)^2\right]\frac{\sin^2\alpha_n}{\alpha_n^2}. \tag{16}$$

We measured the spontaneous emission spectra of the fundamental and third harmonics by using the same observational system around the wavelength of 870 nm, as shown in Fig. 5. The factor a was 8.8×10^{-4} in these measurements, and $\Delta\lambda$ was 0.83 nm at the wavelength of 870 nm. Using equation (16), the calculated values of $f_{\mathrm{m}1}$ and $f_{\mathrm{m}3}$ were 0.696 and 0.762, respectively. On the other hand, the calculated values of $f_{\gamma1}$ and $f_{\gamma3}$ were 0.646 and 0.378, respectively, from equation (10). Then, the products $f_{\gamma1}f_{\mathrm{m}1}$ and $f_{\gamma3}f_{\mathrm{m}3}$ were 0.450 and 0.288. From Fig. 5, the measured values of f were 0.428 for the fundamental harmonic and 0.283 for the third harmonic. The measured and calculated values of the modulation factors are listed in Table 2. These experimental results show that the observation-related evaluation of the modulation factor for the nth harmonic spontaneous emission, which we derived in equation (16), was appropriate.

5. Spectral envelope of the FEL amplification factor

The higher harmonics of the spontaneous emission have the FEL gain, and we have already achieved higher harmonic FEL oscillations by using ETLOK-III, as mentioned in the *Introduction*. Here, we discuss a unique spectrum of the FEL amplification factor for the higher harmonics; this spectrum was based on the optical klystron's spontaneous emission spectrum.

When there is no amplifier in an optical cavity, the spectrum $P(\lambda)$ of a resonant light transmitted through the cavity mirror is given by

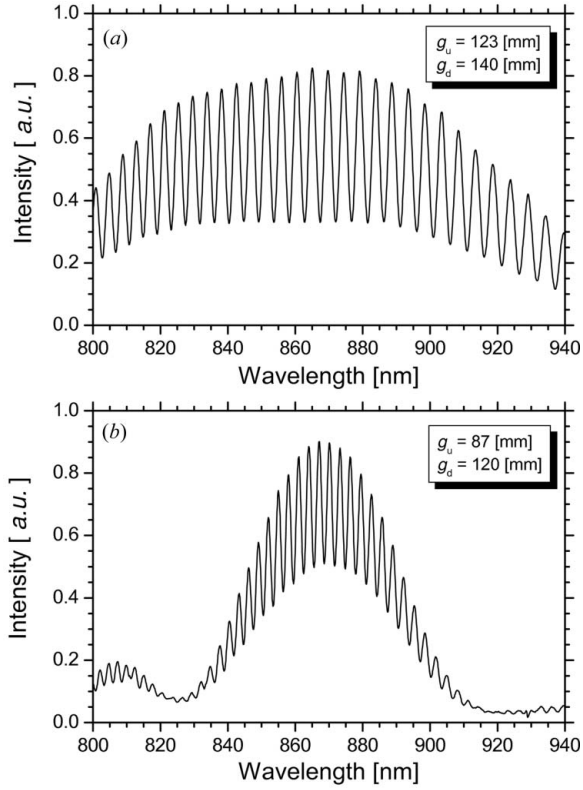

Figure 5
Measured spectra of the fundamental harmonic (*a*) and the third harmonic (*b*) spontaneous emission at the resonant wavelength of ~870 nm in a single-bunch operation. The undulator gaps were 123 mm (K = 2.08) in (*a*) and 87 mm (K = 4.14) in (*b*). The dispersive gaps were 140 mm in (*a*) and 120 mm in (*b*).

$$P(\lambda) = S_{\rm OK}(\lambda)\ \frac{T(\lambda)}{1 - R^2(\lambda)}, \tag{17}$$

where $T(\lambda)$ and $R(\lambda)$ are the transmittance and reflectance of the cavity mirror, respectively. When a small FEL amplification exists and the condition $1 - R^2(\lambda) \ll 1$ holds true, the spectrum $P(\lambda)$ is modified and is described by the following equation,

$$P(\lambda) = S_{\rm OK}(\lambda)\ \frac{T(\lambda)}{1 - R^2(\lambda) - g(\lambda)}, \tag{18}$$

where $g(\lambda)$ is the FEL gain spectrum, and it must satisfy the condition $1 - R^2(\lambda) > g(\lambda)$. The FEL amplification factor $A(\lambda)$ is defined as

$$A(\lambda) = \frac{1 - R^2(\lambda)}{1 - R^2(\lambda) - g(\lambda)}. \tag{19}$$

According to Madey's theorem (Madey, 1979), the small signal FEL gain is proportional to the derivative of the spontaneous emission spectrum with respect to the electron beam energy. Then, the following relationship for $g(\lambda)$ holds,

$$g(\lambda) \propto \frac{\rm d}{{\rm d}\gamma} S_{\rm OK}(\lambda) = \frac{{\rm d}\lambda}{{\rm d}\gamma}\frac{\rm d}{{\rm d}\lambda} S_{\rm OK}(\lambda). \tag{20}$$

Because $S_{\rm OK}(\lambda)$ has a microstructure, $g(\lambda)$ also has a microstructure, including a sine function. In the case of $N_{\rm d} \gg N_{\rm u}$, the rate of change of ${\rm d}S_{\rm OK}/{\rm d}\lambda$ is much larger than that of ${\rm d}\lambda/{\rm d}\gamma$ in the neighborhood of $\lambda_{{\rm R}n}$. The positive envelope of the FEL gain spectrum $g_{\rm en}(\lambda)$ is approximately given as

$$g_{\rm en}(\lambda) \propto \left(\frac{\sin\delta_\lambda}{\delta_\lambda}\right)^2. \tag{21}$$

If we define a parameter Λ_n in the neighborhood of $\lambda_{{\rm R}n}$ as

$$\Lambda_n \equiv \lambda_{{\rm R}n} - \lambda, \qquad \left|\Lambda_n\right| \ll \lambda_{{\rm R}n}/\pi N_{\rm u} n, \tag{22}$$

the following equation for $g_{\rm en}(\Lambda_n)$ holds,

$$\begin{aligned} g_{\rm en}(\Lambda_n) &\cong g_{\rm m}\left[\frac{\sin(\pi N_{\rm u} n \Lambda_n/\lambda_{{\rm R}n})}{\pi N_{\rm u} n \Lambda_n/\lambda_{{\rm R}n}}\right]^2 \\ &\cong g_{\rm m}\left[1 - \frac{(\pi N_{\rm u} n \Lambda_n/\lambda_{{\rm R}n})^2}{3}\right], \end{aligned} \tag{23}$$

where $g_{\rm m}$ is the effective FEL gain, considering the lengthening of the electron bunch that is caused by the bunch heating (Elleaume, 1984*b*). The value of $g_{\rm m}$ approaches the cavity loss when the electron beam current is larger than the threshold current of the FEL oscillation. Using equations (19) and (21), the positive envelope of the FEL amplification factor $A_{\rm en}(\Lambda_n)$ is given in the neighborhood of $\lambda_{{\rm R}n}$ by

$$A_{\rm en}(\Lambda_n) = \frac{1 - R^2}{1 - R^2 - g_{\rm m} + \left(g_{\rm m}\pi^2 N_{\rm u}^2 n^2/3\lambda_{{\rm R}n}^2\right)\Lambda_n^2}. \tag{24}$$

The dependence of the reflectance of the mirror on the wavelength is negligible in the neighborhood of $\lambda_{{\rm R}n}$; thus, the reflectance of the mirror is expressed as R instead of being expressed as $R(\lambda)$. Therefore, it is found that the positive envelope of the FEL amplification factor is characterized by a Cauchy distribution. The width of $A_{\rm en}(\Lambda_n)$ in FWHM, w_n, is given by

$$w_n = \frac{2\lambda_{{\rm R}n}}{\pi N_{\rm u} n}\left[\left(3/g_{\rm m}\right)\left(1 - R^2 - g_{\rm m}\right)\right]^{1/2}. \tag{25}$$

Note that w_n is inversely proportional to the order of a higher harmonic.

To investigate the behavior of the FEL amplification factor for higher harmonics, we generated the fundamental and the third-harmonic oscillations in FELs at wavelengths of around 1530 nm (Sei *et al.*, 2012*c*). Fig. 6 shows the FEL spectra observed for the threshold currents. The cavity loss was evaluated to be 0.13% at wavelengths of ∼1530 nm. Fig. 7 shows the calculated FEL amplification factors that are the ratios of the threshold lasing to the resonant light power at the microstructure peaks in Fig. 6. It is clarified that the envelope of the FEL amplification factors is described by a Cauchy distribution. When the measured data of the FEL amplification rates were fitted with the Cauchy distribution, the widths of the fitting curves were 19.2 nm for the fundamental harmonic and 10.4 nm for the third harmonic in FWHM. The peak heights were 10.3 for the fundamental harmonic and 4.7 for the third harmonic. These parameters of the fitting curves to Cauchy distributions are listed in Table 3. Because the

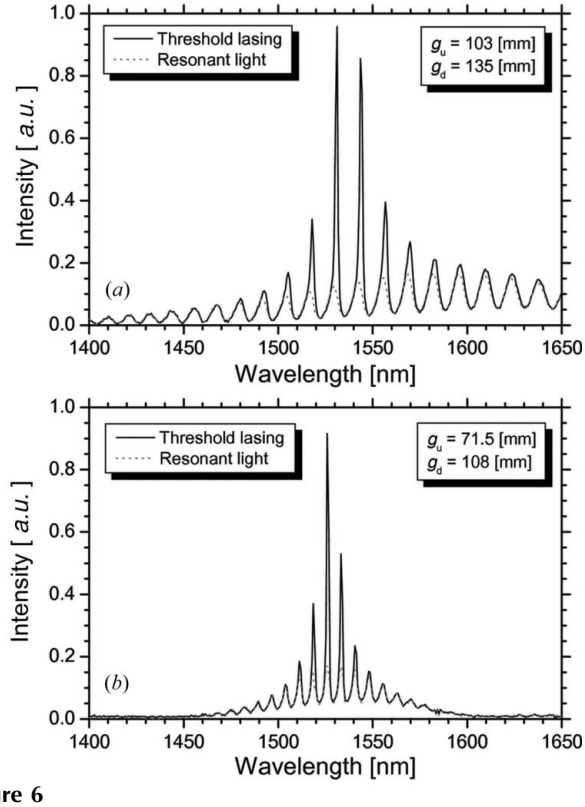

Figure 6
Measured spectra of the fundamental harmonic (*a*) and the third harmonic (*b*) resonant lights at a wavelength of ∼1530 nm in a single-bunch operation. The FEL oscillations were on (solid lines) and off (dotted lines) the threshold at an electron beam current of ∼1.0 mA in (*a*) and 1.6 mA in (*b*). The undulator gaps were 103 mm (K = 3.03) in (*a*) and 71.5 mm (K = 5.60) in (*b*). The dispersive gaps were 135 mm in (*a*) and 108 mm in (*b*).

Table 3
Parameters of Cauchy distributions fitting to the FEL amplification factors for the fundamental and third harmonics.

Order of harmonic, n	Resonant wavelength, λ_{Rn} (nm)	Peak height	FWHM, w_n (nm)
1	1535	10.3	19.2
3	1527	4.7	10.4

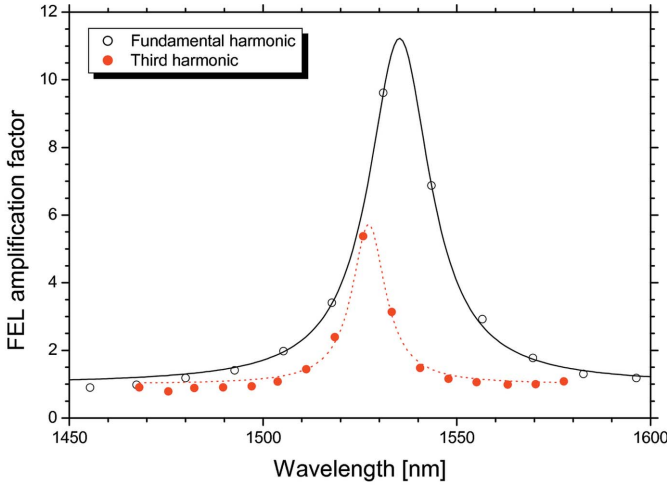

Figure 7
Calculated FEL amplification factors for the fundamental harmonic (open circle) and the third harmonic (solid circle). The solid and dotted lines are the fitting curves to Cauchy distributions.

square-root of the maximum of the FEL amplification factors is inversely proportional to the width, the width for the third harmonic, evaluated by using the measured data of the FEL amplification factors for the fundamental harmonic, was approximately 9.5 nm. This evaluated value is roughly in accord with the measured value of 10.4 nm. Thus, the behavior of the FEL amplification factor for the optical klystron's higher harmonics could be obtained both theoretically and experimentally.

6. Conclusion and discussion

Using the infrared FEL system of the storage ring NIJI-IV, we observed spontaneous emission spectra from an optical klystron, and clarified some unique characteristics pertaining to the higher harmonics. The modulation factor of the spontaneous emission spectrum for the higher harmonics was discussed, and it was shown experimentally that the modulation factor derived by us was appropriate. The microstructure interval of the spontaneous emission spectrum was measured for the higher harmonics, and it was found that the interval at a certain resonant wavelength became narrower as the order of the higher harmonic became larger. Moreover, the envelope of the FEL amplification factor was analytically suggested to be described by a Cauchy distribution. The width of the envelope was experimentally demonstrated to become narrow as the order of the higher harmonic increased.

Application of higher harmonics is a key technique for developing short coherent radiation. Recently, high-peak-power X-ray FELs have been obtained by using self-amplified spontaneous emission (Emma *et al.*, 2010; Pile, 2011). The next goal for developing the light sources will be the development of compact coherent light sources in the extreme-ultraviolet and X-ray regions. Studies of light sources by using higher harmonics, such as a high-gain harmonic generation and an echo-enabled harmonic generation (Yu *et al.*, 2000; Stupakov, 2009), are in their advanced stages throughout the world. The application to higher harmonics to an X-ray FEL lasing is also considered (Schneidmiller & Yurkov, 2012; Dai *et al.*, 2012), and an insertion device of the optical klystron type may be useful for obtaining a high FEL gain there. We expect that the results and conclusions of our present studies on higher harmonics will be applied to the development of compact coherent light sources with a superconductivity linac in the extreme-ultraviolet and X-ray regions.

This study was financially supported by the Budget for Nuclear Research of the Ministry of Education, Culture, Sports, Science and Technology, based on the screening and counselling by the Atomic Energy Commission.

References

Benson, S. V. & Madey, J. M. J. (1989). *Phys. Rev. A*, **39**, 1579–1581.
Billardon, M., Deacon, D. A. G., Elleaume, P., Ortega, J. M., Robinson, K. E., Bazin, C., Bergher, M., Madey, J. M. J., Petroff, Y. & Velghe, M. (1983). *J. Phys. (Paris)*, **44**(C1), 29–71.
Billardon, M., Elleaume, P., Ortega, J. M., Bazin, C., Bergher, M., Velghe, M., Deacon, D. A. G. & Petroff, Y. (1985). *IEEE J. Quant. Electron.* **21**, 805–823.
Brau, C. A. (1990). *Free-Electron Lasers*, p. 64. San Diego: Academic.
Couprie, M. E., Billardon, M., Bazin, C. & Velghe, M. (1989). *Nucl. Instrum. Methods Phys. Res. A*, **285**, 31–42.
Couprie, M. E., Velghe, M., Prazeres, R., Jaroszynski, D. & Billardon, M. (1991). *Phys. Rev. A*, **44**, 1301–1315.
Dai, J., Deng, H. & Dai, Z. (2012). *Phys. Rev. Lett.* **108**, 034802.
Deacon, D. A. G., Billardon, M., Elleaume, P., Ortega, J. M., Robinson, K. E., Bazin, C., Bergher, M., Velghe, M., Madey, J. M. J. & Petroff, Y. (1984). *Appl. Phys. B*, **34**, 207–219.
Elleaume, P. (1984*a*). *J. Phys. (Paris)*, **44**(C1), 333–352.
Elleaume, P. (1984*b*). *J. Phys.* **45**, 997–1001.
Emma, P. *et al.* (2010). *Nat. Photon.* **4** 641–647.
Girard, B., Lapierre, Y., Ortega, J. M., Bazin, C., Billardon, M., Elleaume, P., Bergher, M., Velghe, M. & Petroff, Y. (1984). *Phys. Rev. Lett.* **53**, 2405–2408.
Hama, H., Kimura, K., Hosaka, M., Yamazaki, J. & Kinoshita, T. (1997). *Nucl. Instrum. Methods Phys. Res. A*, **393**, 23–27.
Khan, S., Bakr, M., Höner, M., Huck, H., Molo, R., Nowaczyk, A., Schick, A., Ungelenk, P. & Zeinalzadeh, M. (2011). *Synchrotron Radiat. News*, **24**(5), 18–22.
Kubarev, V. V., Kulipanov, G. N., Shevchenko, O. A. & Vinokurov, N. A. (2011). *J. Infrared Millim. Terahertz. Waves*, **32** 1236–1242.
Labat, M., Hosaka, M., Mochihashi, A., Shimada, M., Katoh, M., Lambert, G., Hara, T., Takashima, Y. & Couprie, M. E. (2007). *Eur. Phys. J. D*, **44**, 187–200.
Litvinenko, V. N. (1988). *Synchrotron Radiat. News*, **1**(5), 18–20.
Litvinenko, V. N. (2003). *Nucl. Instrum. Methods Phys. Res. A*, **507**, 265–273.
Litvinenko, V. N., Park, S. H., Pinayev, I. V. & Wu, Y. (2001). *Nucl. Instrum. Methods Phys. Res. A*, **475**, 195–204.

Litvinenko, V. N., Park, S. H., Pinayev, I. V., Wu, Y., Emamian, M., Hower, N., Morcombe, P., Oakeley, O., Swift, G. & Wang, P. (1999). *Nucl. Instrum. Methods Phys. Res. A*, **429**, 151–158.
Madey, J. M. J. (1979). *Nuovo Cim.* **50**B, 64–88.
Marsi, M., Trovò, M., Walker, R. P., Giannessi, L., Dattoli, G., Gatto, A., Kaiser, N., Guünster, S., Ristau, D., Couprie, M. E., Garzella, D., Clarke, J. A. & Poole, M. W. (2002). *Appl. Phys. Lett.* **80**, 2851–2853.
Neil, G. R., Benson, S. V., Biallas, G., Gubeli, J., Jordan, K., Myers, S. & Shinn, M. D. (2001). *Phys. Rev. Lett.* **87**, 084801.
Pile, D. (2011). *Nat. Photon.* **5**, 456–457.
Prazeres, R., Guyot-Sionnest, P., Ortega, J. M., Jaroszynski, D., Billardon, M., Couprie, M. E., Velghe, M. & Petroff, Y. (1991). *Nucl. Instrum. Methods Phys. Res. A*, **304**, 72–76.
Prazeres, R., Ortega, J. M., Bazin, C., Bergher, M., Billardon, M., Couprie, M. E., Velghe, M. & Petroff, Y. (1988). *Nucl. Instrum. Methods Phys. Res. A*, **272**, 68–72.
Schneidmiller, E. A. & Yurkov, M. V. (2012). *Phys. Rev. ST AB*, **15**, 080702.
Sei, N., Ogawa, H. & Yamada, K. (2009). *Opt. Lett.* **34**, 1843–1845.
Sei, N., Ogawa, H. & Yamada, K. (2010). *J. Phys. Soc. Jpn*, **79**, 093501.
Sei, N., Ogawa, H. & Yamada, K. (2011). *Opt. Lett.* **36**, 3645–3647.
Sei, N., Ogawa, H. & Yamada, K. (2012*a*). *Opt. Express*, **20**, 308–316.
Sei, N., Ogawa, H. & Yamada, K. (2012*b*). *Appl. Phys. Lett.* **101**, 144101.
Sei, N., Ogawa, H. & Yamada, K. (2012*c*). *J. Phys. Soc. Jpn*, **81**, 093501.
Sei, N., Ohgaki, H., Mikado, T. & Yamada, K. (2002). *Jpn. J. Appl. Phys.* **41**, 1595–1601.
Sei, N., Yamada, K. & Ogawa, H. (2007). *Jpn. J. Appl. Phys.* **46**, 3644–3653.
Sei, N., Yamada, K., Ogawa, H. & Yasumoto, M. (2008). *Infrared Phys. Technol.* **51**, 375–377.
Stupakov, G. (2009). *Phys. Rev. Lett.* **102**, 074801.
Takano, S., Hama, H. & Isoyama, G. (1993). *Nucl. Instrum. Methods Phys. Res. A*, **331**, 20–26.
Vinokurov, N. A. & Skrinskii, A. N. (1977). Preprint INP 77–59, Novosibirsk, USSR.
Walker, R. P., Clarke, J. A., Couprie, M. E., Dattoli, G., Eriksson, M., Garzella, D., Giannessi, L., Marsi, M., Poole, M. W., Renault, E., Roux, R., Trovò, M., Werin, S. & Wille, K. (2001). *Nucl. Instrum. Methods Phys. Res. A*, **467–468**, 34–37.
Warren, R. W., Haynes, L. C., Feldman, D. W., Stein, W. E. & Gitomer, S. J. (1990). *Nucl. Instrum. Methods Phys. Res. A*, **296**, 84–88.
Wu, Y. K., Benson, S. V., Li, J., Mikhailov, S. F., Neil, G. & Popov, V. (2008). *Proceedings of the 30th International Free Electron Laser Conference 2008*, Gyeongju, Korea (http://epaper.kek.jp/FEL2008/papers/tucau04.pdf).
Yamazaki, T., Yamada, K., Sugiyama, S., Ohgaki, H., Sei, N., Mikado, T., Noguchi, T., Chiwaki, M., Suzuki, R., Kawai, M., Yokoyama, M., Owaki, K., Hamada, S., Aizawa, K., Oku, Y., Iwata, A. & Yoshiwa, M. (1993). *Nucl. Instrum. Methods Phys. Res. A*, **331**, 27–33.
Yoshikawa, K., Shinzato, T., Yamamoto, Y., Ohnishi, M. & Yamazaki, T. (1994). *Nucl. Instrum. Methods Phys. Res. A*, **358**, 295–299.
Yu, L. *et al.* (2000). *Science*, **289**, 932–935.